DOI: 10.1002/ejic.200600779

Computational Determination of Iron Hyperfine Interactions in Organometallics Using Small Transverse External Magnetic Fields

Israel Nowik*[a] and Rolfe H. Herber[a]

Keywords: Mössbauer spectroscopy / Metallocenes / Quadrupole splitting / Magnetic hyperfine field / External magnetic field perturbation / Iron

A number of organometallic and related iron-containing compounds have been examined by transmission ^{57}Fe Mössbauer spectroscopy in modest (0–2.4 T) magnetic fields in order to determine the sign of the quadrupole-splitting hyperfine parameter (QS) as well as the internal magnetic field in derived paramagnetic solids. A computer program has been developed to extract these parameters from the spectroscopic data. The sign of the QS is found to be positive in the neutral ferrocenoid solids and negative in the derived cationic complexes. The internal hyperfine field makes a positive contribution in the cationic ferrocenoids and a negative contribution in FeF_2 and $Fe(phen)_2(SCN)_2$.

Introduction

Diamagnetic and paramagnetic iron compounds may display ^{57}Fe Mössbauer spectra composed of a pure quadrupole doublet. The quadrupole splitting (QS) of this doublet is given by:

$$QS = \tfrac{1}{2}\, e^2qQ(1 + \tfrac{1}{3}\eta^2)^{1/2}$$

where e^2qQ is the quadrupole interaction and η is the value of the electric field gradient anisotropy [$\eta = (\mathbf{V}_{xx} - \mathbf{V}_{yy})/\mathbf{V}_{zz}$]. It is well known that magnetic fields acting on the Mössbauer absorber nuclei will change the spectra in such a way that the sign of the quadrupole interaction can be obtained. However, perturbations that will yield definite and readily observable results require magnetic fields above 2 T. Such measurements have been carried out in the past and the underlying theory has been worked out to various degrees of approximation.[1]

Here we present a theoretical treatment for the case of an applied magnetic field perpendicular to the γ-ray. The theory contains the diagonalization of the full Hamiltonian for any orientation of the local electric field gradient (EFG) main axis to the magnetic field. For powder samples an averaging over all possible random orientations is performed, taking into account the anisotropy of the Mössbauer recoil-free fraction. A computer program has been developed that uses this theory to least-square fit the simulated spectra to the experimental spectra, yielding the sign of the quadrupole interaction even for the low applied magnetic fields available in most laboratories. In addition to the value of the quadrupole interaction and η, the spectra yield the effective magnetic field acting on the nucleus. In paramagnetic compounds this is not necessarily equal to the applied magnetic field, and yields the value and sign of the induced magnetic internal hyperfine field. For axial cases ($\eta = 0$) the analysis also yields the mean square vibrational anisotropy parameter $N = k^2(\langle x^2_{par}\rangle - \langle x^2_{per}\rangle)$.[2] If the samples studied contain texture effects, the theory will take this into account and determine the fraction aligned in the plane of the absorber. The method is applied to the study of powders of diamagnetic and paramagnetic iron-containing organometallics.

[a] Racah Institute of Physics, The Hebrew University, Jerusalem 91904, Israel
E-mail: nowik@vms.huji.ac.il

Theory

We have chosen the laboratory coordinate system (x, y, z) in which the γ-ray is along the "x" axis, and the magnetic field is in the plane of the absorber, along the "z" axis. The orientation of the randomly distributed axial EFG is along ($\sin\theta\cos\phi$, $\sin\theta\sin\phi$, $\cos\theta$), defined as the local coordinate system z' axis (see Figure 1). For calculating the Mössbauer nuclear level energies and transition probabilities the quantization axis is chosen to be that of the magnetic field, the laboratory "z" axis. This simplifies the considerations of the absorption line intensities' dependence on the direction of the γ-ray.

Thus the Hamiltonian $\mathbf{H}$ for the ^{57}Fe excited level ($I = 3/2$) has the general, non-axial quadrupole form (1):

$$\mathbf{H} = g_{exc}H_{eff}I_z + (e^2qQ/12)[3I_{z'}^2 - I(I+1) + \eta(I_{x'}^2 - I_{y'}^2)] \quad (1)$$

Here the magnetic term is defined in the laboratory system, whereas the quadrupole interaction is in the local coordinate system. In the case of axial symmetry, when $\eta = 0$, the calculation of the matrix elements of the quadrupole

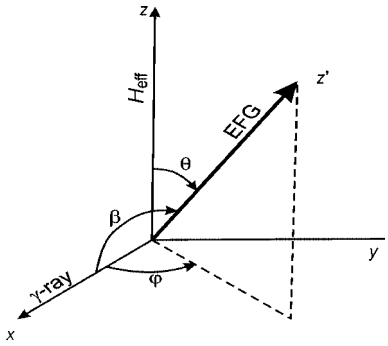

Figure 1. The experimental layout in the laboratory coordinate system. The γ-ray is in the $z = 0$ plane; its direction is chosen to be the x axis so that the absorber is in the $x = 0$ plane.

interaction term in the laboratory coordinate system becomes very simple. The formulas for the matrix elements have all been calculated.[3] The Hamiltonian matrix is real symmetric, and its eigenvalues and eigenvectors do not depend on the angle ϕ, as is also obvious from the symmetry of the experimental situation shown in Figure 1. Thus the diagonalization of this Hamiltonian and that of the ground state (in the particular choice of quantization axis chosen here, no diagonalization is required for the ground state, $I = ½$) yields the energies $E_{exc}(i)$ ($i = 1, 4$) and $E_{gr}(j)$ ($j = 1, 2$) and the corresponding wave functions $|\psi_{exc},i\rangle$ and $|\psi_{gr},j\rangle$, where all depend on H_{eff}, eqQ, and θ. These wave functions are mixtures of pure $|I,m\rangle$ nuclear wave functions. The nuclear transition probabilities for the nuclear magnetic dipole transition operator T_q, where $q = \Delta m = -1, 0, 1$ corresponding to the $\Delta m = 0$ and $\Delta m = \pm 1$ pure nuclear transitions, is given by: $|\langle\psi_{exc},i|T_q|\psi_{gr},j\rangle|^2$. The matrix elements $\langle m_{ex}|T_q|m_{gr}\rangle$ are proportional to the Clebsch–Gordan coefficients yielding the 3:2:1 line intensities for a normal magnetic powder Mössbauer spectrum. As our quantization z axis is at an angle $\pi/2$ relative to the γ-ray, the γ-ray is along an arbitrary chosen "x" axis, and the electric field gradient z' axis is at angle β [$\cos(\beta) = \sin(\theta)\cos(\phi)$] relative to the γ-ray, the total T_{ij} intensity, considering angular dependence of the various nuclear transitions, will be given by the equations in ref.[4] or ref.[5], which leads to (2):

$$T_{ij}(\theta, \phi) = \Sigma_{q=-1,0,1} |\langle\psi_{exc}, i|T_q|\psi_{gr}, j\rangle|^2 P_q \exp(-N\cos^2\beta) \quad (2)$$

Here the constants P_q are: $P_0 = 1$ and $P_{\pm 1} = ½$. The exponent $\exp(-N\cos^2\beta)$ reflects the anisotropy in the recoil-free fraction defined earlier.[2] The Mössbauer spectrum for a perfect powder sample is now given by the double integral over all orientations of the EFG, namely (3):

$$S_P(\omega) = (1/4\pi)\int_{0\to\pi} \sin\theta\, d\theta\, \Sigma_{i,j} L[\omega, \Gamma, E_{ij}(\theta)] \int_{0\to 2\pi} T_{ij}(\theta, \phi)\, d\phi \quad (3)$$

where $L(\omega, \Gamma, E)$ is the Lorentzian Mössbauer absorption line shape, and ω and Γ are the γ-ray energy and the natural absorption line width, respectively. In the case of non-axial symmetry ($\eta \neq 0$), the full Hamiltonian of Equation (1) has to be diagonalized and then the energies and wave functions depend on all three Euler angles of the transformation between the local and the laboratory coordinate system, which makes the situation more complicated and will be discussed below.

The Texture Effect

If intentionally (or unintentionally) the crystallites in the absorber holder are aligned in the plane, namely their local z' axis (Figure 1) is randomly distributed in the $x = 0$ absorber plane, the calculation of the expected Mössbauer spectrum is simplified. In the present case the angle ϕ is fixed to the value ½π, which means that in Equation (2) we have to replace ϕ by ½π ($\cos\phi = 0$), and the formula for the final spectrum (3) takes the form (4):

$$S_{Tex}(\omega) = (1/\pi)\int_{0\to\pi} \Sigma_{i,j} L[\omega, \Gamma, E_{ij}(\theta)]\, T_{ij}(\theta)\, d\theta \quad (4)$$

If the texture effect is partial, then the observed experimental spectrum is a superposition of Equations (3) and (4), namely (5):

$$S_{Total}(\omega) = a\, S_P(\omega) + (1 - a)\, S_{Tex}(\omega) \quad (5)$$

Thus if a texture effect is present it adds only one extra parameter (a) to the least-square fitting procedure.

Non-Axial Quadrupole Interactions

In the general case where $\eta \neq 0$ in Equation (1) one has to transform the electric field gradient second-order tensor expressed as a diagonal matrix ($\mathbf{V}_{x'x'}$, $\mathbf{V}_{y'y'}$, $\mathbf{V}_{z'z'}$) in the local (x', y', z') coordinate system into the (x, y, z) laboratory coordinate system by three Eulerian angles (ϕ, θ, ψ),[6] and one obtains a nondiagonal, though symmetric, matrix ($\mathbf{V}_{ij}$). Then it is necessary to calculate all the matrix elements of the Hamiltonian in Equation (1), which is now a complex, Hermitian matrix. The quadrupole Hamiltonian has now its more general form (6):

$$\mathbf{H}_Q = ½\, \Sigma_{ij}\, \mathbf{V}_{ij}\, Q_{ij} \quad (6)$$

where the nuclear operators are:[7] $Q_{ij} = ½\,(I_i\, I_j + I_j\, I_i) - {}^1/_3\, \delta_{ij}\, I(I + 1)$

If we identify $\mathbf{V}'_{z'z'}$ with $e^2qQ/12$ and $\mathbf{V}$ as the rotational second-order tensor matrix transform of $\mathbf{V}'$, then the matrix elements of $\mathbf{H}_Q$ are as shown in (7):

$$\begin{aligned}
&\langle m\,|\mathbf{H}_Q|\,m\rangle = \mathrm{V}_{zz}\,(3m^2 - I(I+1)) \\
&\langle m+1\,|\mathbf{H}_Q|\,m\rangle = (\mathbf{V}_{xz} - i\mathbf{V}_{yz})\,(2m+1)\,(I(I+1) - m(m+1))^{½} \\
&\langle m+2\,|\mathbf{H}_Q|\,m\rangle = ½\,(\mathbf{V}_{xx} - \mathbf{V}_{yy} - 2i\mathrm{V}_{xy})\,((I(I+1) - \\
&\qquad m(m+1))\,((I(I+1) - (m+1)(m+2)))^{½}
\end{aligned} \quad (7)$$

After diagonalization of the total Hamiltonian it is possible to calculate the associated spectra and average out over all possible orientations of the electric field gradient (z' axis in Figure 1). Here an additional averaging over the angle ψ has to be performed. The angle between the quantization axis and γ-ray is still $\pi/2$. The anisotropy in the recoil-free fraction is now non-axial and the parameter N is not enough to represent the real situation. However we include this term in the program, as it is better than to ignore

it completely. The angle β between the local z' axis and the γ-ray is still $\cos(\beta) = \sin(\theta)\cos(\phi)$, as is obvious from Figure 1. This procedure was converted to two computer programs. One program is very simple, used only for $\eta = 0$, and works very fast (five least-square fit iterations with eight free parameters and 400 points on the unit sphere), within less than a second on an HP AlphaServer DS20E computer. The other program, used for $\eta \neq 0$, also works well, though it consumes much more (several minutes) computing time than the former. In order to test the programs, simulated spectra for various η values (keeping a positive quadrupole interaction QS = 2.5 mm s^{-1} and H_{ext} = 2.4 T) have been calculated and are shown in Figure 2. One observes that for $\eta = 1$ the spectrum is symmetric and for $\eta = 3$ the spectrum is identical to the $\eta = 0$ case but with a negative quadrupole interaction. These observations are in agreement with those expected theoretically, and thus show that the program yields correct results.

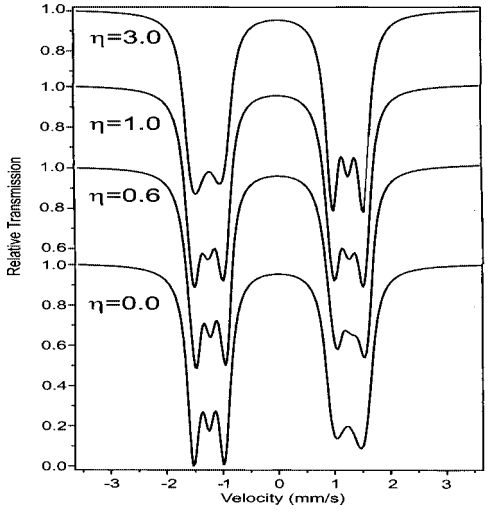

Figure 2. Mössbauer spectra simulations, for various η values, employing the program described in the text.

Paramagnetic Compounds

In the case of paramagnetic compounds, the effective magnetic field (H_{eff}) acting on the nucleus is not equal to the external magnetic field (H_{ext}). H_{ext} can be accurately measured by a diamagnetic compound situated with identical geometry in the field. The unpaired electrons, which produce a fluctuating magnetic field averaged to zero in the absence of an external field, contribute in the presence of an external field at a temperature T the additional term H_p given by (8):

$$H_p = H_{hf}\, B_S(g\mu_B S H_{ext}/kT) \quad (8)$$

where $g\mu_B S$ is the total magnetic moment of the ground state of the magnetic ion (μ_B is the Bohr magneton and g is the gyromagnetic factor), B_S is the spin S Brillouin function, and H_{hf} is the hyperfine magnetic field produced by this electronic state. For $\mu_B H_{ext}/kT << 1$, one can write the simple approximate relation (9):

$$H_p = [g\mu_B(S + 1)H_{hf}/3kT]H_{ext} \quad (9)$$

Namely, the effective field acting on the nucleus is given now by (10):

$$H_{eff} = \{1 + [g\mu_B(S + 1)H_{hf}/3kT]\}H_{ext} \quad (10)$$

In the cases where the magnetic ion has a ground-state Kramers doublet with an effective spin $S = ½$, common in the magnetic organometallics, formula (10) obtains the form (11):

$$H_{eff} = [1 + (g_{eff}\mu_B S H_{hfa}/kT)]H_{ext} \quad (11)$$

where in powders $g_{eff} = {}^1/_3\, g_{\parallel} + {}^2/_3\, g_{\perp}$ and H_{hfa} is a similar average of H_{hf}. Thus a measurement of a paramagnetic compound in an external magnetic field may yield the average value of H_{hf} with its sign (12):

$$H_{hfa} = (kT/g_{eff}\mu_B S H_{ext})(H_{eff} - H_{ext}) \quad (12)$$

In strongly covalent systems, such as diamagnetic organometallics, H_{hf} can be very large and positive. Indeed we observe, for example, in paramagnetic octamethylferrocenium tetrafluoroborate ($OMFc^+BF_4^-$) and decamethylferrocenium hexafluorophosphate ($DMFc^+PF_6^-$), that H_{eff} is much larger than H_{ext}, as will be discussed below.

Results and Discussion

As a test case for the procedure, a sample of FeF_2, containing an impurity (probably $FeF_3{\cdot}3H_2O \approx 10\%$), whose hyperfine interaction parameters are known,[8,9] has been studied. The spectra in zero external magnetic field and in an external field of 2.13 T are displayed in Figure 3. Using the known starting parameters (isomer shift, quadrupole interaction, and saturation magnetic hyperfine field) of both

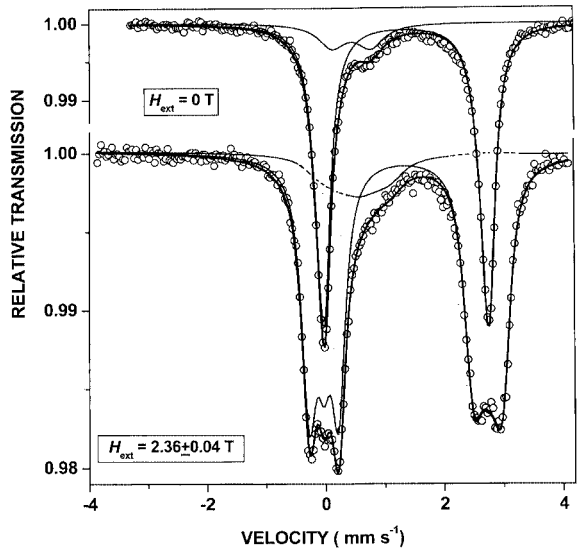

Figure 3. Mössbauer spectra of (predominantly) FeF_2 in H_{ext} = 0 (upper trace) and H_{ext} = 2.36 T (lower trace). The solid curve represents the program least-square fit, yielding the parameters given in Table 1.

Table 1. The hyperfine interaction parameters obtained from the Mössbauer spectra in zero external magnetic field (1) and in a field of 2.13 or 2.35 T (2).

Compound	IS1 ($mm\,s^{-1}$)	QS1 ($mm\,s^{-1}$)	Γ1 ($mm\,s^{-1}$)	IS2 ($mm\,s^{-1}$)	QS2 ($mm\,s^{-1}$)	η	Γ2 ($mm\,s^{-1}$)	H_{eff} (T)	H_{hf} sign (T)
OMFc	0.413(3)	2.512(3)	0.299(2)	0.411(3)	2.505(3)		0.284(4)	2.13(5)	0
$OMFc^+BF_4^-$	0.40(2)	–0.21(2)	0.32(5)	0.40(2)	–0.21		0.32	2.32(9)	38 P
DMFc	0.420(5)	2.478(5)	0.339(2)	0.412(9)	2.473(9)		0.302(2)	2.36(4)	0
$DMFc^+PF_6^-$	0.411(6)	–0.272(6)	0.485(6)	0.416(6)	–0.240(6)		0.420(10)	2.59(14)	46 P
$Fe(phen)_2(SCN)_2$	0.951(2)	2.669(2)	0.30(1)	0.976(3)	–2.587(3)	0.2(1)	0.33(1)	2.07(2)	–28 N
FeF_2[a]	1.35	2.826	0.29	1.35	2.81	0.6(1)	0.29	2.14	–20 N
$Na_2Fe[(CN)_5NO]\cdot 2H_2O$	–0.273(10)	1.711(1)	0.337(4)	–0.275(5)	1.713(5)	0.5(1)	0.302(4)	2.332	

[a] Contains 10% impurity, probably $FeF_3\cdot 3H_2O$.

FeF_2 and $FeF_3\cdot 3H_2O$ (averaged over the two phases[9]), we obtain, from the computer least-square fit, the solid curve shown in the lower trace of Figure 3. The fit to the experimental spectrum is quite satisfactory, and the numerical data, including the hyperfine parameters η, H_{eff}, and H_{hf}, are summarized in Table 1. It is noted that η of FeF_2 is determined to relatively good precision. As both compounds have significant ionic character in the iron–ligand bonding, the magnetic hyperfine fields are negative, and the effective field acting on the metal atom nuclei is smaller than the external field.

Turning next to the application of this methodology to the study of primarily covalent iron organometallics, a typical application of transverse magnetic field measurements to decamethylferrocene is summarized graphically in Figure 4. The upper ME spectrum is in zero applied field and yields the parameters $IS = 0.420 \pm 0.003\ mm\,s^{-1}$ and $QS = +2.478 \pm 0.004\ mm\,s^{-1}$ in good agreement with the previously published values.[10] The line width (Γ, FWHM) = $0.339 \pm 0.002\ mm\,s^{-1}$ is slightly broadened from its theoretical value because of the effect of the long (38 cm) source drive rod. The lower spectrum is that recorded with the same sample in a transverse applied field. The hyperfine parameters obtained from the least-square fit to the above outlined theoretical calculations are: $IS = 0.412 \pm 0.009\ mm\,s^{-1}$, $\Gamma = 0.302 \pm 0.002\ mm\,s^{-1}$, $QS = +2.473 \pm 0.009\ mm\,s^{-1}$, $H_{ext} = 2.36 \pm 0.04$ T, $\eta \leq 0.02$, and $N \leq 0.05$. It is immediately obvious from the lower trace that the peak at negative velocities consists of three lines, while the peak at positive velocities is composed of an asymmetric doublet. Comparing these results with those of Collins and Travis[1] (for ferrocene), it is clear (even visually) that the QS is positive in DMFc, as it is in ferrocene itself.

In order to test the sensitivity of the computer program in determining the sign of the quadrupole interaction, we repeated the measurement in external fields of 0.81, 1.34, 1.86, and 2.34 T. In the case of the lowest field, one notices in Figure 5 that the sign cannot be determined visually, or by measuring the line width of the two components. However the computer program least-square fit yields quite a large difference in χ^2 values between assumed positive and negative quadrupole interactions, with QS consistently positive. An obvious extension of these results is to the paramagnetic decamethyl ferricinium tetrafluoroborate ($DMFc^+BF_4^-$). In zero field, the resonance spectrum consists of a broadened absorption line, which can be fitted to a spin relaxation model calculation and corresponds to IS = $0.401 \pm 0.006\ mm\,s^{-1}$ and QS = $-0.272 \pm 0.006\ mm\,s^{-1}$. This spectrum is shown in the upper trace of Figure 6. When

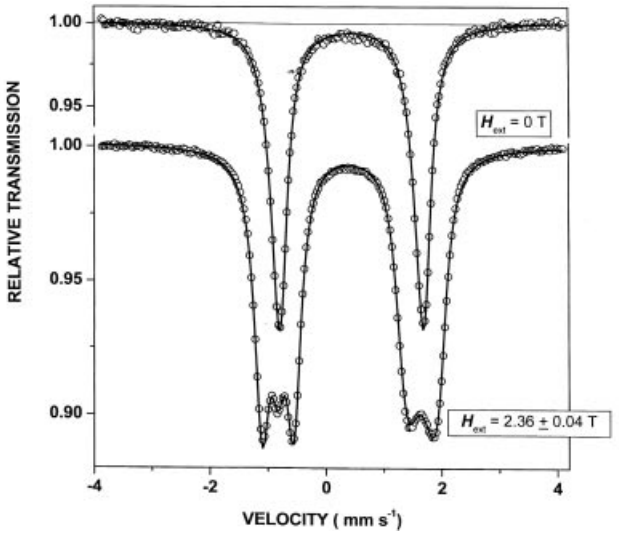

Figure 4. Mössbauer spectra of decamethylferrocene, in $H_{ext} = 0$ (upper trace) and $H_{ext} = 2.36$ T (lower trace). The solid curve represents the program least-square fit, yielding the parameters given in Table 1.

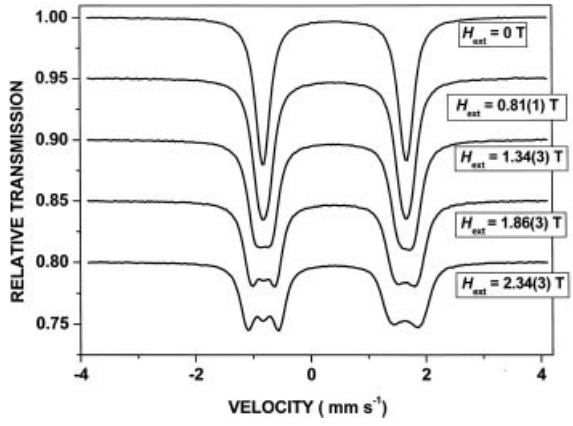

Figure 5. Mössbauer spectra of decamethylferrocene in a series of external magnetic field values. The ordinate offsets were arbitrarily fixed at 5% but all spectra were accumulated under identical conditions.

this sample is examined in a transverse magnetic field the resonance line is broadened to give an asymmetric doublet, as shown in the lower trace of Figure 6. The internal field is $H_{eff} = 2.58 \pm 0.03$ T. The value of the QS was frozen to its zero-field value of –0.272 mm s^{-1}. The negative sign of the quadrupole interaction is derived not only from the zero-field spectrum (Figure 6), but also from the fact that the χ^2 value of the computer fit is consistently smaller for a negative value of this parameter than for a positive value also in the in-field spectrum. It should be noted that H_{eff} for the cationic complex, under identical conditions, is larger than that observed for the neutral complex by ≈0.19 T, which, according to Equation (12), leads to a positive value for the internal magnetic hyperfine field, $H_{hf} \approx +38$ T.

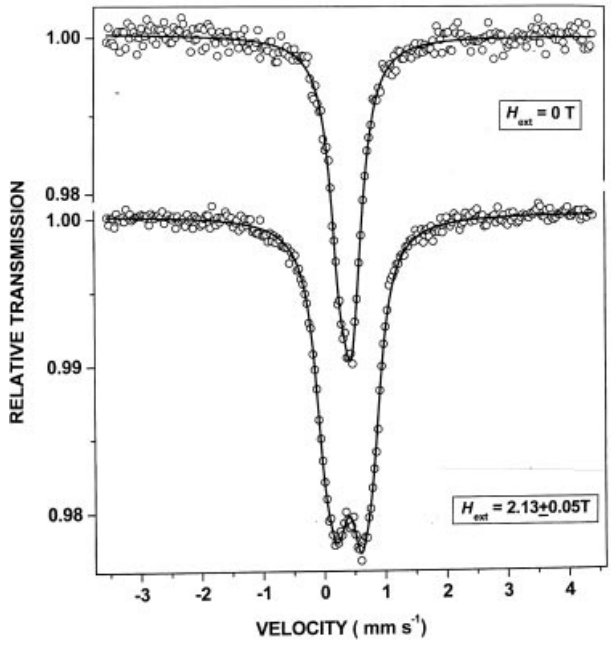

Figure 6. Mössbauer spectra of decamethylferrocenium tetrafluoroborate ($DMFc^+BF_4^-$), in $H_{ext} = 0$ (upper trace) and $H_{ext} = 2.36$ T (lower trace). The solid curve represents the program least-square fit, yielding the parameters given in Table 1.

A comparable set of experiments has been carried out with ^{57}Fe OMFc and ^{57}Fe $OMFc^+BF_4^-$, and the parameters extracted from the corresponding Mössbauer spectra are included in Table 1. As in the case of the DMFc complexes, the QS parameter is clearly positive in the neutral compound and negative in the cationic homologue.

We observe in paramagnetic $OMFc^+BF_4^-$ that H_{eff} is significantly larger than H_{ext}, and yields a magnetic hyperfine field H_{hf} (assuming that $g_{eff}\mu_B S$ is about 1 μ_B) of about +40 T. Such large positive hyperfine fields have been previously observed and interpreted as due to orbital contributions to the hyperfine field.[11,12] Once H_{hf} is estimated, one can use this value for the analysis of the zero external field Mössbauer spectra from which spin relaxation rates can be derived, using a simple spin ½ up down formula.[13] The reduced hyperfine interaction parameters from the least-square fitting of the various Mössbauer spectra are all summarized in Table 1.

The above experiments were carried out on ^{57}Fe-enriched ferrocenoid complexes in which the shape of the electric field around the metal atom is expected to be oblate, because of the C_{5v} symmetry of the ring ligands.

These measurements have been further extended to an iron complex in which the shape of the electric field around the metal atom is expected to be prolate, of which $Fe(phen)_2(SCN)_2$ (phen = 1,10 phenanthroline) is a representative example. This compound has been extensively studied by Mössbauer effect spectroscopy[14,20] in view of its interesting high spin–low spin transition at ca. 175 K. At room temperature the iron is in a high-spin state and has an effective moment of ca. 5 μ_B, indicating the presence of four unpaired electrons ($S = 2$). The two SCN ligands occupy *cis* positions, and hence the asymmetry parameter $\eta \neq 0$. These experiments were carried out with natural abundance iron, so that relatively long data acquisition times (up to 72 h) were required to record statistically significant data. The brass sample cavity in this case was $0.4 \times 0.4 \times 1$ cm^3, and typically holds 0.7–1.0 mmol of solid. As before, the pole piece gap was 0.6 cm. A typical data set is summarized graphically in Figure 7, where again the zero-field resonance spectrum is shown in the upper trace, and the in-field absorbance in the lower. Although the magnetic splitting is smaller than that observed in the ferrocenoid complexes, it is clear that in an applied field of 2.36 ± 0.04 T the absorbance at negative velocities is due to an asymmetric doublet, while that at positive velocities arises from a triplet, in agreement with the existence of a negative QS. The least-square fit analysis yields the hyperfine interaction parameters given in Table 1. The striking result is that in the present case, H_{eff} is smaller (!) than the external field,

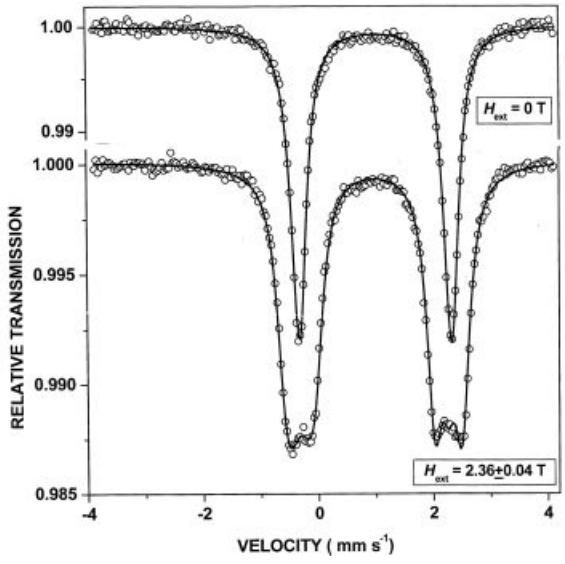

Figure 7. Mössbauer spectra of bis(phenanthroline)bis(thiocyanato)iron(II), in $H_{ext} = 0$ (upper trace) and $H_{ext} = 2.36$ T (lower trace). The solid curve represents the program least-square fit, yielding the parameters given in Table 1.

namely the induced internal hyperfine field is negative and leads according to Equation (10) to the value of $H_{hf} \approx -28$ T.

An example of a compound in which η is expected to be equal or close to zero is provided by $Na_2Fe[(CN)_5NO]\cdot 2H_2O$, SNP, which has again been thoroughly investigated by Mössbauer techniques,[15,21] in part because of its interesting optical properties and ease of preparation of high-purity single crystals. An early high-precision study of very thin samples has been published by Grant et al.[16] Single-crystal X-ray diffraction studies[17] have shown that the local site symmetry is C_{4v} and the space group is P_{nnm} and $\eta \leq 0.04$. A magnetic field experiment carried out on a finely crushed powder sample is summarized graphically in Figure 8 and the derived hyperfine parameters are included in Table 1. From Figure 8 it is evident that the quadrupole splitting (1.713 ± 0.005 mm s^{-1} at room temperature) is positive, in consonance with the results reported by Grant.[18] The η value obtained from the data processed by the $\eta \neq 0$ program is 0.5, although the χ^2 value is not very much smaller than for $\eta = 0$.

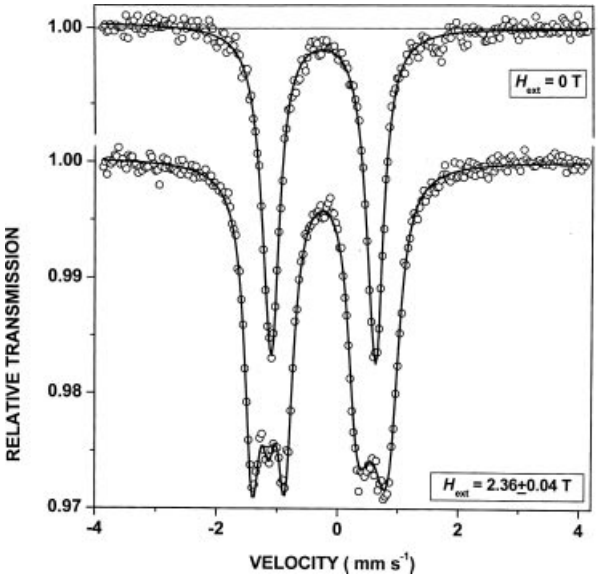

Figure 8. Mössbauer spectra of sodium nitroprusside dihydrate [Fe^{II} in $H_{ext} = 0$ (upper trace) and $H_{ext} = 2.36$ T (lower trace)]. The solid curve represents the program least-square fit, yielding the parameters given in Table 1.

Conclusions

Using a standard laboratory electromagnet having 3-cm pole pieces and operating at about 7 A, in conjunction with transmission Mössbauer spectroscopy it has been possible to determine the sign of the quadrupole splitting in a series of organometallic iron compounds at room temperature. In addition, the application of a complete diagonalization program of the full Hamiltonian for powder samples averaging over all possible random orientations makes it possible to extract the internal hyperfine field in both diamagnetic and paramagnetic complexes. While the use of enriched (^{57}Fe) samples reduces the required data acquisition time, even natural abundance samples employing in the order of 1 mmol of iron complex permits the acquisition of statistically reliable parameter information in reasonable data-acquisition times. The quadrupole splitting is positive in diamagnetic complexes such as OMFc, DMFc, and Fe(phen)$_2$(SCN)$_2$ (as it is in ferrocene itself), and negative in the associated one-electron oxidation products. In addition, corresponding data are presented for FeF_2.

Experimental Section

A sample of natural abundance FeF_2, produced by microwave irradiation of $Fe(NO_3)_3\cdot 9H_2O$ in the presence of $BMIBF_4$,[8,19] was generously made available to us by Prof. A. Gedanken of Bar Ilan University and used as received. Samples of ^{57}Fe-enriched decamethylferrocene (DMFc), decamethylferrocenium hexafluorophosphate ($DMFc^+PF_6^-$), octamethylferrocene (OMFc), and octamethylferrocinium tetrafluoroborate ($OMFc^+BF_4^-$) were generously made available by Prof. H. S. Schottenberger of the University of Innsbruck. Bis(phenanthroline)bis(thiocyanato)iron(II) [Fe(phen)$_2$(SCN)$_2$] was prepared by literature methods[9] and its purity was checked by FTIR measurements. Sodium nitroprusside [$Na_2Fe(CN)_5NO\cdot 2H_2O$][10] was taken from high-purity single-crystal material. All solids were ground with Pyrex powder and mixed with BN to assure the absence of texture-induced asymmetry in the spectra. The powdered enriched Fe^{57} samples were transferred to a rectangular brass holder of 6 mm width and 2 mm thickness (unless otherwise noted), having a sample cavity of 0.08 cm^3, which will hold (typically) about 0.4–0.6 mmol of an organometallic solid. The sample space was windowed with 5 N Al foil and the holder assembly clamped between the pole pieces of an electromagnet. The DC electromagnet used in this study was a Newport Instruments model 369 having gap-adjustable shaped pole faces, which allowed variable field intensities to be investigated. The standard pole piece gap was 0.6 cm. Normal operating conditions were 55 V and 6–7 A at room temperature. The Mössbauer effect measurements were carried out in transmission geometry, with the 100 mCi ^{57}Co (Rh) source mounted on a 38 cm long stainless steel tube driven by a standard triangular wave velocity drive. As was noted above, this arrangement leads to only a small (less than 0.05 mm s^{-1}) broadening of the resonance lines. Spectrometer calibration was effected in magnet geometry ($H = 0$) by standard α-Fe absorption, and all IS are reported with respect to the centroid of this spectrum.

Data analysis was effected in the usual manner, by the above-described programs. These computer programs are available upon request from the corresponding author.

Acknowledgments

The authors are indebted to Prof. H. Schottenberger for providing samples of the enriched compounds examined in this study, and to O. Levy for the preparation of high-purity Fe(phen)$_2$(SCN)$_2$.

[1] R. L. Collins, J. C. Travis in *Mössbauer Effect Methodology* (Ed.: I. J. Gruverman), Plenum Press, New York, **1967**, vol. 3, p. 123, and references therein.
[2] V. I. Goldanskii, E. F. Makarov in *Chemical Applications of Mössbauer Spectroscopy* (Eds.: V. I. Goldanskii, R. H. Herber), Academic Press, **1968**, p. 105.
[3] E. Matthias, W. Schneider, R. M. Steffen, *Phys. Rev.* **1962**, *125*, 261.

[4] W. T. Oosterhuis, G. Lang, *Phys. Rev.* **1969**, *178*, 439.
[5] J. P. Zory, *Phys. Rev. A: At. Mol. Opt. Phys.* **1965**, *140*, 1401.
[6] H. Goldstein (Ed.), *Classical Mechanics*, Addison-Wesley, **1956**, pp. 107–109.
[7] S. Ofer, I. Nowik, S. G. Cohen, in *Chemical Applications of Mössbauer Spectroscopy* (Eds.: V. I. Goldanskii, R. H. Herber), Academic Press, **1968**, p. 442.
[8] G. K. Wertheim, H. J. Guggenheim, D. N. E. Buchanan, *Phys. Rev.* **1967**, *169*, 465–470; A. R. Champion, R. W. Vaughan, H. G. Drickamer, *J. Chem. Phys.* **1967**, *47*, 2583.
[9] D. G. Karraker, P. K. Smith, *Inorg. Chem.* **1992**, *31*, 1118–1120.
[10] R. H. Herber, I. Nowik, V. Kahlenberg, H. Kopacka, H. Schottenberger, *Eur. J. Inorg. Chem.* **2006**, 3255–3260.
[11] K. Ono, M. Shinohara, A. Ito, N. Sakai, M. Suenaga, *Phys. Rev. Lett.* **1970**, *24*, 770.
[12] H. Andres, E. L. Baminaar, J. M. Smith, N. A. Eckert, P. L. Holland, E. Münck, *J. Am. Chem. Soc.* **2002**, *124*, 3012.
[13] I. Nowik, H. H. Wickman, *Phys. Rev. Lett.* **1966**, *17*, 949–951.
[14] P. Gütlich in *Chemical Mössbauer Spectroscopy* (Ed.: R. H. Herber), Plenum Press, New York, **1984**, ch. 2, pp. 27ff and references cited therein; W. M. Reiff, G. J. Long, *Inorg. Chem.* **1974**, *13*, 2150–2153.
[15] See the discussion, in: N. N. Greenwood, T. C. Gibb, *Mössbauer Spectroscopy*, Chapman Hall Ltd., London, **1971**, pp. 90 and 182–187.
[16] R. W. Grant, R. M. Housley, U. Gonser, *Phys. Rev.* **1969**, *178*, 523–530.
[17] P. T. Manorahan, W. C. Hamilton, *Inorg. Chem.* **1963**, *2*, 1043–1047.
[18] R. W. Grant in *Mössbauer Effect Methodology* (Ed.: I. J. Gruverman), Plenum Press, New York, **1966**, vol. 2, pp. 23–38.
[19] D. S. Jacob, L. Bitton, J. Grinblat, I. Felner, Y. Koltypin, A. Gedanken, *Chem. Mater.* **2006**, *181*, 3162–3168.
[20] E. König, K. Madeja, *Inorg. Chem.* **1967**, *6*, 48–55 and refs. therein; P. Ganguli, P. Gütlich, E. W. Müller, *J. Chem. Soc., Dalton Trans.* **1981**, 441–446; W. A. Baker, H. M. Bobonich, *Inorg. Chem.* **1964**, *3*, 1184–1188.
[21] R. W. Grant, R. M. Housley, U. Gonser, *Phys. Rev.* **1969**, *178*, 523–530; R. M. Housley, R. W. Grant, U. Gonser, *Phys. Rev.* **1969**, *178*, 514.

Received: August 23, 2006
Published Online: October 27, 2006

